Self-Assembly of 10-*μ*m-Sized Objects into Ordered Three-Dimensional Arrays

Thomas D. Clark, Joe Tien, David C. Duffy, Kateri E. Paul, and George M. Whitesides*

Contribution from the Department of Chemistry and Chemical Biology, Harvard University, 12 Oxford Street, Cambridge, Massachusetts 02138

Received March 9, 2001

Abstract: This paper describes the self-assembly of small objects—polyhedral metal plates with largest dimensions of 10 to 30 *μ*m—into highly ordered, three-dimensional arrays. The plates were fabricated using photolithography and electrodeposition techniques, and the faces of the plates were functionalized to be hydrophobic or hydrophilic using self-assembled monolayers (SAMs). Self-assembly occurs in water through capillary interactions between thin films of a hydrophobic liquid (a liquid prepolymer adhesive) coated onto the hydrophobic faces of the plates; coalescence of the adhesive films reduces the interfacial free energy of the system and drives self-assembly. By altering the size and surface-patterning of the plates, the external morphologies of the aggregates were varied. Curing the adhesive furnished mechanically stable aggregates that were characterized by scanning electron microscopy (SEM). For assemblies formed by plates partially composed of a sacrificial material, a subsequent etching step furnished fully open, three-dimensional microstructures. This work validates the use of capillary interactions for three-dimensional mesoscale self-assembly in the 10-*μ*m-size regime and opens new avenues for the fabrication of complex, three-dimensional microscructures.

Introduction

Three-dimensional (3-D) structures with micrometer-scale features are difficult to fabricate. This difficulty notwithstanding, the characteristics of these structures—large volumetric densities of components, large ratios of interior surface area to volume, and the potential for generating complex internal shapes—make them attractive as candidate materials with photonic band gap properties,[1] as components of heat exchangers, as supports for catalysis or chromatography, and ultimately, perhaps, as platforms around which to build 3-D microelectronic systems.[2] Strategies for fabrication based on self-assembly provide new routes to 3-D arrays of small objects: they create stable constructs having a low level of defects, and they can be applied to many structures and materials.[3−11] Here, we demonstrate that

self-assembly using capillary interactions can form large, regular arrays ("crystals") of components with largest dimensions of 10−30 *μ*m.

Previous studies concerning self-assembly of small objects have dealt mainly with colloidal crystals—ordered arrays of particles having dimensions in the range of 1 nm to 1 *μ*m. Examples of colloidal crystal formation in natural systems include the geological production of opals[12] and the biological crystallization of proteins and viruses.[13,14] Synthetic assemblies of monodispered colloids with sizes ranging from 0.1 to 1 *μ*m are of interest in the preparation of photonic band gap materials,[15,16] while superlattices of semiconducting (quantum dots) and metallic nanocrystals 1−100 nm in size are being studied for potential electronic, optical, optoelectronic, and magnetic device applications.[17,18] The attractive forces used in the preparation of synthetic colloidal crystals include molecular recognition,[19] dipolar,[20,21] electrostatic,[22,23] light-based,[24] mag-

(1) Yablonovitch, E. *J. Opt. Soc. Am. B: Opt. Phys.* **1993**, *10*, 283−295.

(2) Marchand, P. J.; Krishnamoorthy, A. V.; Yayla, G. I.; Esener, S. C.; Efron, U. *J. Parallel Distrib. Comput.* **1997**, *41*, 20−35.

(3) Terfort, A.; Bowden, N.; Whitesides, G. M. *Nature* **1997**, *386*, 162−164.

(4) Terfort, A.; Whitesides, G. M. *Adv. Mater.* **1998**, *10*, 470−473.

(5) Gracias, D. H.; Tien, J.; Breen, T. L.; Hsu, C.; Whitesides, G. M. *Science* **2000**, *289*, 1170−1172.

(6) Bowden, N.; Arias, F.; Deng, T.; Whitesides, G. M. *Langmuir* **2001**, *17*, 1757−1765.

(7) Bowden, N. B.; Weck, M.; Choi, I. S.; Whitesides, G. M. *Acc. Chem. Res.* **2001**, *34*, 231−238.

(8) Cohn, M. B.; Kim, C. J.; Pisano, A. P. Self-Assembling Electrical Networks: An Application of Micromachining Technology. In *Digest of Technical Papers*; TRANSDUCERS '91; 1991 International Conference on Solid-State Sensors and Actuators, San Francisco, CA.; 1991; IEEE: New York, NY, 1991; 91CH2817−5, 490−493.

(9) Yeh, H.-J. J.; Smith, J. S. *IEEE Photonics Technol. Lett.* **1994**, *6*, 706−708.

(10) Hosokawa, K.; Shimoyama, I.; Miura, H. *Sens. Actuators* **1996**, *A57*, 117−125.

(11) Rothemund, P. W. K. *Proc. Natl. Acad. Sci. U.S.A.* **2000**, *97*, 984−989.

(12) Harder, H. *Neues Jahrb. Mineral., Monatsh.* **1995**, 121−126.

(13) Poon, W. C. K. *Phys. Rev. E: Stat. Phys., Plasmas, Fluids, Relat. Interdiscip. Top.* **1997**, *55*, 3762−3764.

(14) Pieranski, P. *Contemp. Phys.* **1983**, *24*, 25−73.

(15) Xia, Y.; Gates, B.; Yin, Y.; Lu, Y. *Adv. Mater.* **2000**, *12*, 693−713.

(16) Blanco, A.; Chomski, E.; Grabtchak, S.; Ibisate, M.; John, S.; Leonardo, S. W.; Lopez, C.; Meseguer, F.; Miguez, H.; Mondia, J. P.; Ozin, G. A.; Toader, O.; Van Driel, H. M. *Nature* **2000**, *405*, 437−440.

(17) Murray, C. B.; Kagan, C. R.; Bawendi, M. G. *Annu. Rev. Mater. Sci.* **2000**, *30*, 545−610.

(18) Sun, S.; Murray, C. B.; Weller, D.; Folks, L.; Moser, A. *Science* **2000**, *287*, 1989−1992.

(19) Mann, S.; Shenton, W.; Li, M.; Connolly, S.; Fitzmaurice, D. *Adv. Mater.* **2000**, *12*, 147−150.

(20) Poulin, P.; Stark, H.; Lubensky, T. C.; Weitz, D. A. *Science* **1997**, *275*, 1770−1773.

(21) Wickman, H. H.; Korley, J. N. *Nature* **1998**, *393*, 445−447.

(22) Larsen, A. E.; Grier, D. G. *Nature* **1997**, *385*, 230−233.

(23) Messina, R.; Holm, C.; Kremer, K. *Phys. Rev. Lett.* **2000**, *85*, 872−875.

netic,[25] entropic,[26,27] and capillary interactions.[28] Most of these studies have examined close-packed arrays of monodispersed spheres, although a few assemblies of non-spherical colloids have been reported.[29-35]

Of late, a number of groups have begun to examine the self-assembly of non-spherical components with dimensions larger than those of colloids. Cohn et al. have experimented with the self-assembly of hexagonal plates $\sim$1 mm in diameter using mechanical agitation and gravity.[8] When placed on a slightly concave diaphragm and agitated by a loudspeaker, the plates self-assembled into a two-dimensional (2-D) lattice. Smith and co-workers have pursued a related strategy, fluidic self-assembly (FSA), for the integration of microelectronic device elements and substrates made of incompatible materials.[9,36] In one system reported, trapezoidal GaAs blocks dispensed from a carrier liquid filled trapezoidal holes patterned on a silicon wafer. For a number of years, physicists have used computation and experiments to study the flow and self-ordering behavior of granular matter—including sand, spherical beads, and disks—for a variety of applications such as the development of new technology for powder processing.[37] Recently, we described the formation of ordered, 2- and 3-D arrays of small objects via mesoscale self-assembly (MESA)—self-assembly using forces that operate over distances comparable to the lateral dimensions of the components being assembled.[3-5,7] In our initial work, we examined mm-sized subunits that interact through capillary forces extending over millimeter ranges.[3-5,7] Application of MESA to the fabrication of functional devices such as photonic band gap materials and self-assembling microelectonic systems, however, will require miniaturization of the components to the submillimeter- and, in some cases, submicrometer-scales. Recent reports from this laboratory[7] and from Hosokowa and co-workers[10] have demonstrated two-dimensional MESA at the fluid—fluid interface, using components with largest dimensions of 100-600 μm. In the present study, we show that self-assembly based on capillary interactions can form large, ordered, three-dimensional arrays of 10-μm-sized objects.

Here, the objects that self-assemble are polyhedral, metallic pieces that are fabricated by photolithography; this type of fabrication is broadly generalizable to other shapes, sizes, and materials, and can generate large numbers of indistinguishable units. The faces of the plates are functionalized to be either hydrophobic or hydrophilic using self-assembled monolayers (SAMs), and a hydrophobic liquid (a photocurable or thermally curable adhesive) is deposited selectively onto the hydrophobic faces. When these liquid-coated plates are suspended in water and agitated, collisions between them allow contact and coalescence of the adhesive films; this coalescence minimizes the interfacial area between the adhesive and water and drives self-assembly. By controlling the geometries and surface properties of each face, we can tailor the strengths and directionalities of interactions between pieces.

To simplify fabrication, this study examined the self-assembly of hexagonal plates in which all of the rectangular sides were either hydrophobic or hydrophilic; both hexagonal faces had the same wettability. The use of hexagonal plates limits the number of slip planes in the resulting aggregates: arrays of hexagonal plates have three (two translational, one rotational); arrays of cubes, in contrast, have six (three translational, three rotational). We expect fewer slip planes to correlate with fewer defects in the self-assembled arrays and with increased rates of assembly. We describe each type of plate using the notation $M_1(\sim R_1)|\mathbf{M_2(\sim R_2)}|M_1(\sim R_1)$, where M_1 and R_1 refer to the underlying metal and surface functionalities, respectively, of the faces, M_2 and R_2 refer to those of the sides, and bold type refers to hydrophobic surfaces that are coated with adhesive.

Results

Figure 1 summarizes a typical process used to fabricate plates with defined hydrophobic faces, to deposit a hydrophobic liquid on these faces, and to allow the pieces to self-assemble. A thin film of silver on a silicon wafer served as a cathode and, later, as a sacrificial layer. Electrodeposition of gold on the silver film through lithographically fabricated hexagonal holes in photoresist generated hexagonal gold plates. Dissolution of the silver film after electrodeposition released plates that presented gold at all of the faces. To make plates with gold sides and with top and bottom chromium or platinum-coated faces, we evaporated chromium or platinum followed by gold onto the silver before lithography. We then electrodeposited gold followed by evaporation of chromium or platinum on the plates (Figure 1a).

After fabrication, we modified the surface chemistry of the pieces using SAMs.[38] Treatment of plates having Cr/Cr_2O_4 on top and bottom faces and gold exposed at the sides with hexadecanethiol ($HS(CH_2)_{15}CH_3$; HDT) generated $Cr(\sim OH)|\mathbf{Au(\sim CH_3)}|Cr(\sim OH)$ plates: a hydrophobic CH_3-terminated SAM coated the gold surfaces, while a hydrophilic native oxide coated the chromium surfaces. We prepared hydrophobic $\mathbf{Au(\sim CH_3)|Au(\sim CH_3)|Au(\sim CH_3)}$ plates by treating plates that lacked chromium coatings with hexadecanethiol.

For the preparation of hexagonal plates having hydrophobic top and bottom faces and hydrophilic sides, we examined two different strategies. Our first approach employed orthogonal SAMs on gold and chromium. Thiol ($-SH$) endgroups coordinate to gold, and phosphonate ($-PO_3H_2$) endgroups coordinate a variety of native metal oxides such as Cr/Cr_2O_4.[39] Treatment of plates, having Cr/Cr_2O_4 on top and bottom faces and gold exposed at the sides, with $HS(CH_2)_{11}PO_3H_2$ covered the chromium surfaces with a SAM that exposed moderately hydrophobic thiol (or, after oxidation, disulfide) endgroups ($\theta_a(H_2O) \approx 50°$), and the gold surfaces were covered with one that exposed hydrophilic phosphonate endgroups ($\theta_a(H_2O) = 0°$); in our notation, this treatment generated $Cr(\sim \mathbf{SH})|Au(\sim PO_3H_2)|Cr(\sim \mathbf{SH})$ plates. In our second approach, we ex-

(24) Burns, M. M.; Fournier, J. M.; Golovchenko, J. A. *Science* **1990**, *249*, 749-754.

(25) Hwang, Y. H.; Wu, X. I. *Phys. Rev. E: Stat. Phys., Plasmas, Fluids, Relat. Interdiscip. Top.* **1994**, *49*, 3102-3108.

(26) Eldridge, M. D.; Madden, P. A.; Frenkel, D. *Nature* **1993**, *365*, 35-37.

(27) Frenkel, D. *Physica A* **1999**, *263*, 26-38.

(28) Denkov, N. D.; Velev, O. D.; Kralchevsky, P. A.; Ivanov, I. B.; Yoshimura, H.; Nagayama, K. *Nature* **1993**, *361*, 26.

(29) Wang, Z. L.; Harfenist, S. A.; Vezmar, I.; Whetten, R. L.; Bentley, J.; Evans, N. D.; Alexander, K. B. *Adv. Mater.* **1998**, *10*, 808-812.

(30) Wang, Z. L.; Harfenist, S. A.; Whetten, R. L.; Bentley, J.; Evans, N. D. *J. Phys. Chem. B* **1998**, *102*, 3068-3072.

(31) Korgel, B. A.; Fitzmaurice, D. *Adv. Mater.* **1998**, *10*, 661-665.

(32) Wang, Z. L. *Mater. Charact.* **1999**, *42*, 101-109.

(33) Nikoobakht, B.; Wang, Z. L.; El-Sayed, M. A. *J. Phys. Chem. B* **2000**, *104*, 8635-8640.

(34) Mann, S.; Davis, S. A.; Hall, S. R.; Li, M.; Rhodes, K. H.; Shenton, W.; Vaucher, S.; Zhang, B. J. *J. Chem. Soc., Dalton Trans.* **2000**, 3753-3763.

(35) Mbindyo, J. K. N.; Reiss, B. D.; Martin, B. R.; Keating, C. D.; Natan, M. J.; Mallouk, T. E. *Adv. Mater.* **2001**, *13*, 249-254.

(36) For commercial applications of FSA, see: http://www.alientechnology.com.

(37) Mehta, A. *Granular Matter: An Interdisciplinary Approach*; Springer-Verlag: New York, 1994.

(38) Ulman, A. *Chem. Rev.* **1996**, *96*, 1533-1554.

(39) Gao, W.; Dickinson, L.; Grozinger, C.; Morin, F. G.; Reven, L. *Langmuir* **1996**, *12*, 6429-6435.
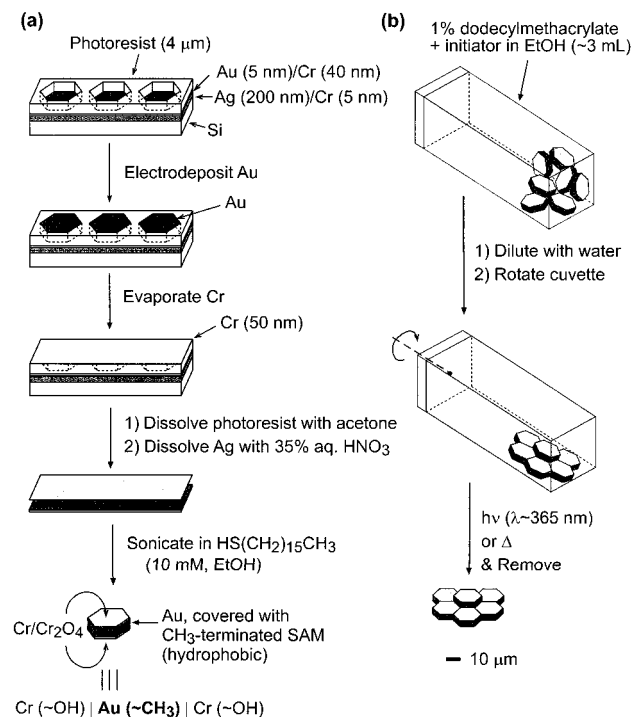
Figure 1. Fabrication and self-assembly of 10-μm-sized Cr(∼OH)|**Au-(∼CH₃)**|Cr(∼OH) plates. (a) Electrodeposition of gold through patterned photoresist on an electrode of Si/SiO₂/Cr/Ag/Cr/Au formed gold plates. Evaporation of chromium and dissolution of the photoresist in acetone, and of the silver film with nitric acid, released the plates as a sheet from the underlying silicon substrate. Sonication of the plates in ethanol and subsequent filtration removed residual thin films of chromium that held plates together. Treatment of the plates in an ethanolic solution of HS(CH₂)₁₅CH₃ formed a hydrophobic SAM on the gold; the Cr/Cr₂O₄ faces remained hydrophilic. (b) Approximately 10⁵ plates were placed in ethanol in a glass cuvette, and ∼30 μL of either a photocurable or thermally curable adhesive that served as lubricant during self-assembly was added to the cuvette. Slow addition of water diluted the ethanol, overflowed the cuvette, and precipitated the adhesive selectively onto the hydrophobic faces of the plates. Axial rotation of the cuvette provided the agitation that allowed self-assembly to proceed. After assembly, curing the adhesive by exposure to UV radiation or heat provided mechanically stable arrays that could be removed for examination.

ploited the differential coordination of isocyanide and thiol functionalities to gold and platinum surfaces.[40,41] Isocyanide (−NC) endgroups coordinate to both gold and platinum, while thiol (−SH) endgroups can displace isocyanides from gold but not from platinum.[40,41] Treatment of plates, having platinum on the top and bottom faces and gold exposed at the sides, with butane isocyanide (CN(CH₂)₃CH₃; BIC) covered the platinum and gold surfaces with a hydrophobic CH₃-terminated SAM. Subsequent treatment with mercaptohexadecanoic acid (HS-(CH₂)₁₅CO₂H) displaced the hydrophobic BIC monolayer on gold with an alkanethiolate SAM that exposed hydrophilic carboxylic acid endgroups but left intact the BIC monolayer on platinum. In our notation, this treatment generated **Pt(∼CH₃)**|Au(∼CO₂H)|**Pt(∼CH₃)** plates.

A typical assembly started with ∼10⁵ plates suspended in water in a cuvette, with a thin film of hydrophobic adhesive on the hydrophobic faces of each plate. Collisions between adhesive-coated faces induced by axial rotation of the cuvette
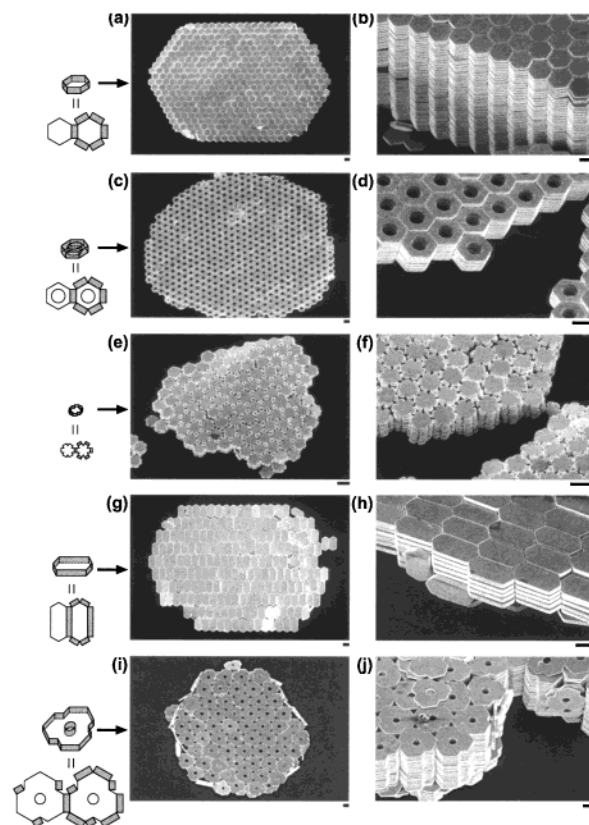
(40) Hickman, J. J.; Laibinis, P. E.; Auerbach, D. I.; Zou, C.; Gardner, T. J.; Whitesides, G. M.; Wrighton, M. S. *Langmuir* **1992**, *8*, 357−359.
(41) Martin, B. R.; Dermody, D. J.; Reiss, B. D.; Fang, M.; Lyon, L. A.; Natan, M. J.; Mallouk, T. E. *Adv. Mater.* **1999**, *11*, 1021−1025.

Figure 2. A variety of Cr(∼OH)|**Au(∼CH₃)**|Cr(∼OH) plates—(a) and (b) hexagons; (c) and (d) hexagons with holes; (e) and (f) stars; (g) and (h) elongated hexagons; (i) and (j) indented hexagons—self-assembled into multilayered, ordered arrays. The scale bar refers to 10 μm, and shading refers to the location of adhesive on each piece.

allowed the liquid films to merge; this merging oriented and juxtaposed the hydrophobic faces of the plates. Each type of plate assembled within a few days into a set of arrays with a characteristic morphology that reflected the pattern of hydrophobic faces for that type of plate. After the self-assembly reached completion, curing the adhesive with light or heat locked the assemblies in place.[42] Control experiments underscored the importance of the hydrophobic adhesive in the self-assembly process. When we rinsed the arrays with ethanol prior to curing the adhesive, the arrays dissociated into individual plates, presumably due to dissolution of the uncured adhesive. In addition, experiments performed with hydrophilic Au(∼PO₃H₂)|Au(∼PO₃H₂)|Au(∼PO₃H₂) plates (made by treatment of gold plates with HS(CH₂)₁₁PO₃H₂) did not result in formation of arrays.

The most crystalline assemblies arose from Cr(∼OH)|**Au-(∼CH₃)**|Cr(∼OH) plates (Figures 2 and 3b). Here, the adhesive was isolated on the sides of the plates. Arrays that self-assembled from these pieces consisted of multilayered stacks that extended further in the hexagonal plane than in the direction perpendicular to it. These stacks were internally well-ordered and externally crystalline, with defined crystal faces characteristic of a hexagonal lattice. By examining the aggregates under a micro-

(42) In our initial experiments, we used a photocurable adhesive as described in the Experimental Section. Since ultraviolet light is unlikely to penetrate deeply into multilayered assemblies such as those shown in Figures 2 and 3, some adhesive in the interior of these assemblies likely remained uncured. When we attempted to use this same adhesive for the experiments described in Figure 4, the assemblies often broke apart during the subsequent etching step. For this reason we ultimately chose to use a thermally curable adhesive in order to achieve uniform curing throughout the arrays. See the Experimental Section for details.

(a)

6 μm I

(b)
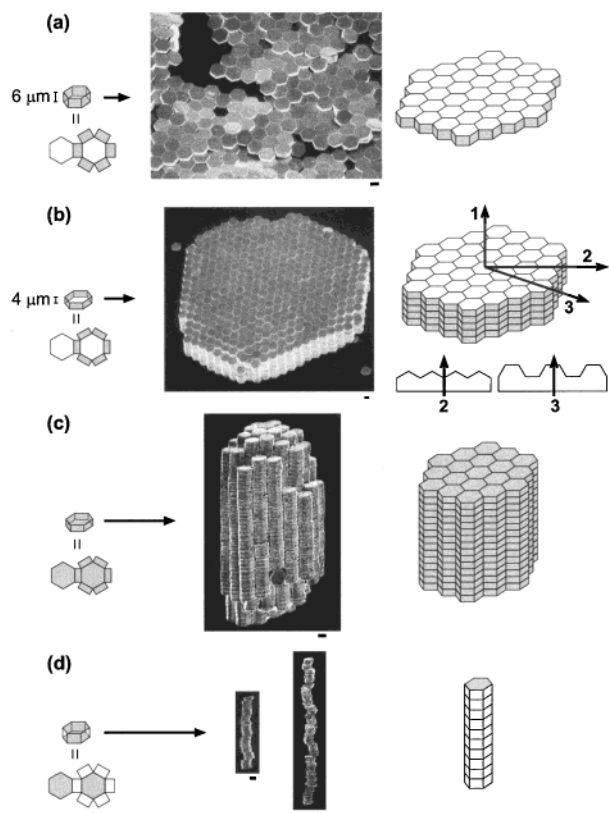
4 μm I

(c)

(d)

Figure 3. The geometry and pattern of edge/face functionalization of hexagonal plates determines the shape of the resulting self-assembled arrays. The scale bar denotes 10 μm; shading refers to the location of adhesive on each piece. (a) Cr($\sim$OH)|**Au($\sim$CH₃)**|Cr($\sim$OH) plates (6-μm thick) assembled into monolayers. (b) Cr($\sim$OH)|**Au($\sim$CH₃)**|Cr-($\sim$OH) plates (4-μm thick) assembled into multilayers. (c) **Au-($\sim$CH₃)|Au($\sim$CH₃)|Au($\sim$CH₃)** plates (4-μm thick) assembled into bundles of rods. (d) **Cr($\sim$SH)**|Au($\sim$PO₃H₂)|**Cr($\sim$SH)** plates (6-μm thick, left) and **Pt($\sim$CH₃)**|Au($\sim$CO₂H)|**Pt($\sim$CH₃)** plates (4-μm thick, right) both assembled into rods.

scope at various times during the course of a single experiment, we observed that the assembly process leading to these multilayers took place in two distinct phases. Within the first few seconds of an experiment, each suspension of plates organized itself into small unilamellar arrays oriented randomly with respect to one another; these arrays were typically composed of $\sim$10$-$100 pieces each and presumably formed through association of individual plates. Agitation for extended periods ($\geq$1 day) allowed the monolayers to disentangle and coalesce into much larger arrays that consisted of $\sim$10⁴$-$10⁵ pieces each; at this stage further agitation did not induce any observable condensation of these arrays into larger crystals. This latter phase of the assembly process is reminiscent of recrystalization events that occur in polycrystalline solids.[43]

These results were independent of the exact geometry of the assembling pieces: hexagons (Figure 2, a$-$d), stars (Figure 2, e,f), elongated hexagons (Figure 2, g,h), and indented hexagons (Figure 2, i,j) all self-assembled into stacks of close-packed planes that were aligned to one another. Even plates that could not tile the plane completely$-$for example, stars and indented hexagons$-$self-assembled into highly ordered structures. We believe that the remarkably good lateral alignment between close-packed planes resulted from capillary interactions involv-

ing adhesive exposed along the interstices in each plane: that is, at the gaps between plates in a plane.

Hydrophobic **Au($\sim$CH₃)|Au($\sim$CH₃)|Au($\sim$CH₃)** plates fully coated with adhesive also formed internally well-ordered arrays (Figure 3c). The external morphologies of these aggregates, however, were very different from those of arrays of Cr($\sim$OH)|**Au($\sim$CH₃)**|Cr($\sim$OH) plates. First, these crystals extended further along the axis perpendicular to the hexagonal plane than in the in-plane directions. Second, these arrays were not externally crystalline. External crystal faces indicative of a hexagonal lattice were absent, and the tops and bottoms of these arrays were not flat. These changes in morphology were accompanied by a different mechanism for formation of arrays. Here, each suspension initially organized into rods, which then bundled together into crystals of $\sim$10⁴ pieces each.

Monolayers (Figure 3a) formed from 6-μm-thick Cr-($\sim$OH)|**Au($\sim$CH₃)**|Cr($\sim$OH) plates, presumably due to the increased stability afforded by a greater hydrophobic contact area relative to the corresponding 4-μm thick pieces (Figure 2a). Single rods (Figure 3d) formed from both 6-μm-thick **Cr($\sim$SH)**|Au($\sim$PO₃H₂)|**Cr($\sim$SH)** plates and 4-μm-thick **Pt($\sim$CH₃)**|Au($\sim$CO₂H)|**Pt($\sim$CH₃)** plates; the similarity of these aggregates established the expected hydrophobicity of the BIC monolayer on platinum and validated the use of orthogonal SAMs on gold and platinum in selectively derivitizing subunits for mesoscale self-assembly. Neither the monolayers nor the single rods were as well-ordered as the multilayers. In the case of the single rods, many of the plates were misaligned with respect to each other. When we slowly rotated a cuvette that contained either monolayers or single rods, we observed (using a microscope) that these arrays often disassembled when they collided with each other or with the walls of the vessel. The mechanical weakness of monolayers, sheets, and rods allows collisions to cause disassembly, and limits the sizes of the arrays.

As a further demonstration of the power of this strategy for self-assembly, we prepared a three-dimensional, open-lattice microstructure using a combination of additive (self-assembly) and subtractive (sacrificial) processes (Figure 4). We fabricated metal/polymer composite plates using a variation of the strategy outlined in Figure 1. The cathode, consisting of a silicon wafer coated with aluminum, chromium, and gold, was patterned with toroidal holes using the negative chemical amplification resist SU-8.[44] After photolithography, the SU-8 formed a hydrophobic cross-linked polymer that served as a mask for the sequential electrodeposition of gold, silver, and gold into the holes. Evaporation of gold and chromium onto the plates, dissolution of the underlying aluminum layer, and treatment with HDT yielded composite circular plates consisting of Cr-($\sim$OH)|**Au($\sim$CH₃)|Ag($\sim$CH₃)|Au($\sim$CH₃)**|Cr($\sim$OH) rings surrounding a central post of SU-8.

Upon self-assembly, the circular plates formed a multilayered hexagonal lattice (Figure 4a). Because circles cannot completely tile a plane, the resulting assemblies contained pores formed by the gaps between circular plates in each plane. After curing the adhesive, treatment of the assemblies with aqueous nitric acid dissolved the electrodeposited silver layer in each plate and yielded a fully open lattice three-dimensional microstructure (Figure 4a). Following a similar procedure, we also prepared terraced rod-shaped structures consisting of stacked gold rings spaced by central posts of SU-8 (Figure 4b).

(43) Dini, J. W. *Electrodeposition: The Materials Science of Coatings and Substrates*; Noyes Publications/William Andrew Publishing: LLC: Norwich, NY, 1993.

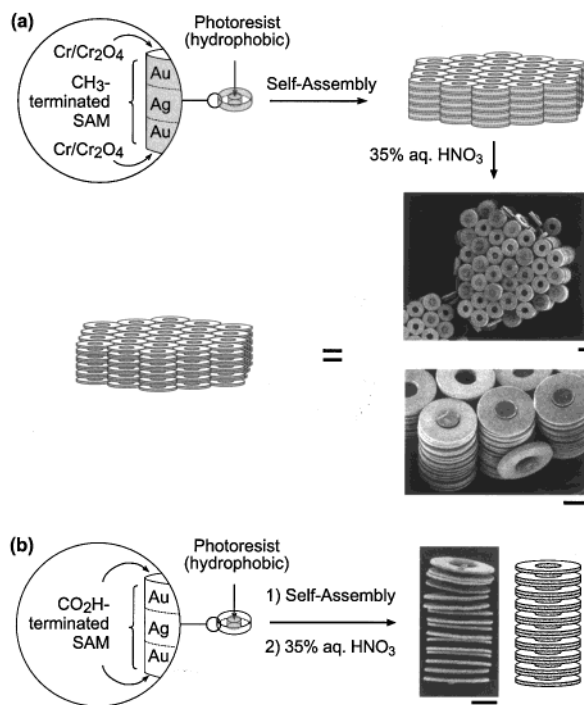(44) Lorenz, H.; Despont, M.; Fahrnl, N.; LaBianca, N.; Renaud, P.; Vettiger, P. *J. Micromech. Microeng.* **1997**, *7*, 121$-$124.

Figure 4. (a) Metal/polymer composite plates each consisting of a Cr($\sim$OH)|**Au**($\sim$**CH₃**)|**Ag**($\sim$**CH₃**)|**Au**($\sim$**CH₃**)|Cr($\sim$OH) ring surrounding a central post of the hydrophobic cross-linked photoresist SU-8 were fabricated using a variation of the electrodeposition strategy depicted in Figure 1. The circular plates self-assembled into a multilayered hexagonal lattice containing pores formed by the gaps between circles in each plane. Treatment of the assemblies with aqueous nitric acid dissolved the electrodeposited silver layer in each circular plate and yielded a fully open lattice three-dimensional structure. (b) Circular plates each consisting of a Au($\sim$CO₂H)|Ag($\sim$CO₂H)|Au-($\sim$CO₂H) ring surrounding an SU-8 post self-assembled into rods through capillary interactions between the exposed regions of the hydrophobic posts. Dissolution of the silver layer in each plate yielded a terraced rod-shaped microstructure.

Discussion

We rationalize the morphology of the aggregates obtained in these studies by using an analysis adapted from the study of crystal growth. Objects with hexagonal symmetry can pack in regular arrays that possess three symmetry axes: an axis with six-fold symmetry oriented perpendicular to the plane of the hexagons (axis **1** in Figure 3b) and two two-fold axes that lie within that plane (axes **2** and **3**). The different morphologies pictured in Figure 3 arise from variations of the extensions of the arrays along these axes. Extension of an array along an axis correlates with the area of hydrophobic faces that are normal to that axis. For plates with hydrophobic sides, nearly all of the hydrophobic area lies perpendicular to the hexagonal plane. A crystal face normal to one of the in-plane symmetry axes (axis **3** in Figure 3b) possesses greater surface area than a face normal to the other in-plane axis (axis **2**). Thus, arrays of these hexagons are thickest along **3** and thinnest out of the plane (along axis **1**). In contrast, plates with all faces hydrophobic, or with only top and bottom faces hydrophobic, are thickest along **1**, and thinner along **2** and **3**.

Defects in these crystals consist mainly of two types: misalignment between sheets of plates and misalignment of individual pieces. The first type of defect constitutes slip along one of the translational slip axes inherent in hexagonal arrays. These defects are especially common if, as in the case of indented hexagons (Figure 2, i,j), the plates can pack in the

plane in more than one way. Elimination of this redundancy would require us to fabricate pieces that do not have flat top and bottom faces; we are currently investigating ways of accomplishing this type of fabrication. The second type of defect may represent a possible limit to the regularity of arrays that use only one force to effect self-assembly. Minimization of this type of defect requires an appropriate choice of agitation; agitation that is too strong or too weak results in misalignment of individual pieces. Alternatively, self-assembly that uses two orthogonal interactions—one in the plane, and one perpendicular to the plane—should eliminate misalignment of this sort.[45]

We estimated the number of defects by counting the misaligned pieces when we examined the arrays using a scanning electron microscope. The density of defects was low ($\sim$0.1$-$1% of plates) and appeared by microscopy to be localized mainly at the surface of the arrays. We used diffraction to characterize order in one case: that of the hexagons with holes shown in Figure 2, c,d. The absence of diffraction, or weak diffraction, would have suggested slip between planes. When light from a laser illuminated one of these aggregates, a hexagonal array of dots emerged, with up to third-order diffraction spots clearly visible. This result shows that the amount of slip in these crystals is small. We could not assess the number of vacancies in the arrays by using microscopy or diffraction.

Conclusions

The results presented here constitute the first demonstration of the self-assembly of non-spherical objects at the 10-μm-scale, and validate the application of MESA to 3-D fabrication in this size regime. Our strategy separates the preparation of a 3-D structure into two distinct parts: the fabrication of the individual units, and their self-assembly. Here, the structure of the assembling unit—the composition of the faces, their surface chemistries, and the thickness of the adhesive layers coating them—tailors the directionality and strength of interactions between pieces and determines the structure of the assembly. The use of capillary forces to achieve self-assembly of 10-μm-sized plates, where the size of the cohering faces was as small as 2 μm (Figure 2, e,f), demonstrates that capillarity can provide a practical basis for self-assembly at this scale.

The principal advantage of this strategy is that, compared with those techniques currently used to fabricate 3-D structures— micromachining,[46] stereolithography,[47] 3-D printing,[47] assembly by robotic placement of individual parts, and holographic lithography—[48]self-assembly is simple and can accommodate a wide variety of materials. Self-assembly also allows access to complex microstructures (Figure 4) that would be difficult to prepare using conventional techniques of microfabrication.

One clear path for further development of these 3-D arrays is the self-assembly of objects with dimensions smaller than 10 μm. Because capillary forces become stronger relative to other forces at smaller size scales,[46] our approach to 3-D self-assembly should extend to the submicrometer scale; the fabrica-

(45) The assembly shown in Figure 3c contains an interesting example of the second class of defect. Here, an individual plate can be seen occupying a gap in a column of hexagons, with its hexagonal faces lying parallel rather than perpendicular to axis **1**. This type of defect is rare and likely arises from the uniform hydrophobicity of the **Au**($\sim$**CH₃**)|**Au**($\sim$**CH₃**)|**Au**($\sim$**CH₃**) pieces used in this experiment, which enables the hexagonal and rectangular faces of the pieces to interact with one another through capillary bonding.

(46) Frazier, A. B.; Warrington, R. O.; Friedrich, C. *IEEE Trans. Ind. Electron.* **1995**, *42*, 423$-$430.

(47) Calvert, P.; Crockett, R. *Chem. Mater.* **1997**, *9*, 650$-$663.

(48) Campbell, M.; Sharp, D. N.; Harrison, M. T.; Dennlng, R. G.; Turberfleld, A. J. *Nature* **2000**, *404*, 53$-$56.

tion of the individual pieces, and the functionalization of their surfaces, appears to be the most difficult aspect of this method of fabrication. Another possibility for future work involves the incorporation of electrical connections in the array.[2,3,5,8,9,49]

Experimental Section

General. All chemicals and solvents were used as obtained from the indicated source. Silicon wafers (3 in., test grade, 13−17 mils, any orientation, 1−10 Ωcm) were obtained from Silicon Sense (Nashua, NH). Chromium, silver, gold, platinum, and aluminum evaporation sources were obtained from Alfa Aesar or Materials Research Corp. Hexadecanethiol and mercaptohexadecanoic acid were obtained from Aldrich. Positive photoresists and developers (SJR5440 and 1808 photoresists; 453 and 351 developers) were obtained from Shipley (Marlboro, MA), and the negative photoresist SU-8-5 was obtained from Microchem Corp. (Newton, MA). Propyleneglycol methyl ether acetate (PGMEA) was obtained from Aldrich. Gold (Techni-25E) and silver (Techni E-2) electroplating solutions were obtained from Technic, Inc. (Cranston, RI). Dodecylmethacrylate was obtained from Polysciences, Inc. (Warrington, PA), and benzoin isobutyl ether, 1,6-hexanediol diacrylate, and benzoyl peroxide were obtained from Aldrich. Absolute ethanol was obtained from Pharmco (Brookfield, CT), and hexanes were obtained from VWR Scientific.

Preparation of Substrates. Silicon wafers were typically cleaned for ~3 min in an oxygen plasma and then coated with the indicated thickness of metal using an electron beam evaporator.[50]

Substrates used in the preparation of the pieces shown in Figures 2−4 were as follows: Figures 2 and 3a, 3b, and 3d (left): (Si/SiO₂/Cr(5 nm)/Ag(200 nm)/Cr(50 nm)/Au(5 nm)); Figure 3d (right): (Si/SiO₂/Ti(200 nm)/Pt(50 nm)/Au(20 nm)); Figure 3c: (Si/SiO₂/Cr(5 nm)/Ag(200 nm)); Figure 4a: (Si/SiO₂/Al(200 nm)/Cr(15 nm)/Au(6 nm)); Figure 4b: (Si/SiO₂/Ti(200 nm)Au/(5 nm)).

Photolithography. Photolithography[50] was performed in a class 100 cleanroom in the absence of ambient ultraviolet light using a Suss MJB 3 mask aligner in contact mode with a 350-W mercury lamp. We obtained the chrome/soda lime photomasks used for photolithography from Advance Reproductions (North Andover, MA).

Substrates used in the preparation of pieces shown in Figures 2 and 3 were primed by immersion for 10 min in 2 mM ethanolic solution of 90:10 hexadecanethiol/mercaptohexadecanoic acid to promote adhesion of the photoresist. We then cleaned the substrates by rinsing them with cleanroom-grade acetone followed by 18 MΩ water, and dried them under a stream of nitrogen. Wafers were typically coated with SJR5440 (Shipley) by spinning at 500 rpm for 5 s and then accelerating to 4000 rpm for over ~1 s and spinning an additional 30 s to give a 4 μm-thick film. We placed the wafers on a hot-plate set at 105 °C, baked them for 5 min, then removed them and allowed them to cool for ~30 sec. The wafers were exposed for 4 s for every 1 μm thickness of photoresist, with the lamp set at 10 mW cm⁻² (λ = 405 nm). We developed the wafers with 453 developer (Shipley).

Substrates used in the preparation of the pieces shown in Figure 4 were not primed prior to spin coating and were subjected directly to the cleaning process described above. We coated the wafers with SU-8-5 by spinning at 500 rpm for 5 s and then accelerating to 3500 rpm for over ~1 s and spinning an additional 15 s to give a 5 μm-thick film. The wafer was then baked 1 min at 65 °C and 3 min at 90 °C, then exposed as above. The resist was postbaked for 3 min at 65 °C and 5 min at 90 °C and developed with PGMEA.

Electrodeposition. Prior to electrodeposition, we cleaned the substrates patterned with SJR5440 photoresist for 5 min in a UV/ozone cleaner to remove the SAM primer; unprimed substrates patterned with SU-8-5 were subjected to electrodeposition without cleaning. For electrodeposition of gold, we used a gold sulfite bath (Techni-25E, 1

Tr oz Au gal⁻¹, Technic, Inc.) at 60 °C with a platinum anode. The solution was stirred at 300 rpm, and the current density was maintained at 1 mA cm⁻²; under these conditions a 1 μm thickness of gold formed in ~16 min. For electrodeposition of silver, we used a silver cyanide bath (Techni E-2, 9 Tr oz Ag gal⁻¹, Technic, Inc.) at room temperature with a silver anode. The solution was stirred at 200 rpm, and the current density was held at 5 mA cm⁻²; under these conditions a 1 μm thickness of silver formed in ~3 min. Using a mechanical profilometer, we found that the thickness of the electrodeposited metal typically varied by ±10% over the surface of a 3-in. wafer.

Isolation and Derivitization of the Pieces. After electrodeposition, a thin film of chromium or platinum was evaporated on the top of pieces if required. We liberated the pieces from the wafer by dissolving the sacrificial layer. Sacrificial layers of silver, aluminum, and titanium were dissolved using 35% aqueous HNO₃ at room temperature, 20% w/v aqueous NaOH at 60 °C, and 5% aqueous HF at 32 °C, respectively.[51] After rinsing away the etchant with water, we sonicated the plates in ethanol to break apart the residual thin films of metal that held the plates together. We agitated the suspension of plates using a vortex mixer, allowed the heavy plates to settle, and decanted the residual thin flakes of metal; repetition of this procedure 4−5 times yielded nearly pure metal plates. The plates were then filtered through a Nylon filter mesh having 53-μm square openings (SpectraMesh, Spectrum Laboratories, Inc.).

We formed alkanethiolate SAMs on the pieces by suspending them in a 2 mM ethanolic solution of the appropriate thiol, followed by incubation for several hours at room temperature. Orthogonal isocyanide and alkanethiolate SAMs on platinum and gold, respectively,[40] were formed using the procedure of Mallouk and co-workers.[41]

Self-Assembly. In a typical experiment, ~10⁵ plates were suspended in 3 mL of ethanol and transferred to a 1 cm × 1 cm × 3 cm glass cuvette; ~30 μL of either a photocurable (96:2:2 w/w/w dodecyl-methacrylate/benzoin isobutyl ether/1,6-hexanediol diacrylate)[3] or thermally curable (85:14.5:0.5 w/w/w dodecyl methacrylate,/1,6-hexanediol diacrylate/benzoyl peroxide) adhesive was then added to the cuvette, and the ethanol was stirred until the adhesive had fully dissolved. We then allowed the pieces to settle into one corner of the cuvette and, using a Pasteur pipet, withdrew nearly all of the ethanol/adhesive solution, leaving only enough to cover the pieces (~50 μL). Water was added slowly to the pieces, precipitating the adhesive mixture selectively onto the hydrophobic surfaces of the plates and causing the pieces to aggregate. We continued to add water (~50 mL) to rinse away all of the excess ethanol and adhesive. After rinsing, the cuvette contained the liquid-coated plates and 3 mL of water, to which we added ~50 μL of concentrated ammonium hydroxide to promote ionization of the glass surface and prevent the pieces from adhering to the walls of the cuvette.

The cuvette was then rotated at a ~10° tilt above the horizontal at 100−200 rpm for 1−3 days. This rotation caused the aggregated pieces to tumble and provided the agitation that allowed the self-assembly to proceed. After assembly, the suspension of pieces was deoxygenated by sparging with N₂ and exposed to UV radiation (λ ≈ 365 nm for ~1 h) or heat (80 °C for 18 h) to polymerize the adhesive. The arrays were then mechanically stable and could be removed and examined by scanning electron microscopy.

(49) Sliwa, J. W., Jr. U.S. Patent 5,075,253, 1991.

(50) Madou, M. *Fundamentals of Microfabrication*; CRC Press LLC: Boca Raton, FL, 1997.

(51) Kern, W.; Deckert, C. A. In *Thin Film Processes*; Vossen, J. L., Kern, W., Eds.; Academic Press: San Diego, 1978; pp 401−496.